

Optics Letters

Intelligent open-set MIMO recognition in OWC using a Siamese neural network

YINAN ZHAO,^{1,2} CHEN CHEN,^{1,4} HAILIN CAO,¹ ZHIHONG ZENG,^{1,5} MIN LIU,¹ AND HARALD HAAS³

Received 2 October 2024; revised 7 November 2024; accepted 25 November 2024; posted 26 November 2024; published 6 December 2024

Multiple-input multiple-output (MIMO) technology, a core component of 6G, has been widely adopted in optical wireless communication (OWC) systems. Accurate recognition of different MIMO types is essential for MIMO selection and demodulation. In this Letter, we propose an open-set MIMO recognition method for OWC systems using a Siamese neural network (SNN). Simulation results show that the SNN significantly outperforms other recognition approaches, including convolutional neural networks (CNNs) and traditional machine learning techniques. For SNN-based recognition, over 90% accuracy is achieved with training based on only nine fixed sampling points in both 2×2 and 4×4 MIMO-OWC systems. © 2024 Optica Publishing Group. All rights, including for text and data mining (TDM), Artificial Intelligence (Al) training, and similar technologies, are reserved.

https://doi.org/10.1364/OL.543826

In recent years, wireless communication has seen significant growth in both usage and importance [1]. As the available radio frequency spectrum is limited, an attractive alternative to radio frequency is optical wireless communication (OWC), which offers the advantage of abundant spectrum and high security [2]. However, despite the numerous advantages of OWC systems, their modulation bandwidth, when using commercially available light-emitting diodes (LEDs), is typically limited to a few MHz [3,4]. One promising solution to overcome this limitation is the implementation of multiple-input multiple-output (MIMO) technology, which is widely recognized for its ability to significantly enhance data transmission speed, coverage, and resilience against multi-path fading [5]. By integrating MIMO with high spectral efficiency modulation schemes, the data rate of OWC systems can be increased to several Gbit/s [6]. Additionally, MIMO-OWC systems offer the benefit of achieving high data rate transmission without requiring additional transmit power or bandwidth, making them an efficient solution for overcoming bandwidth constraints [7].

The most popular MIMO schemes in OWC include repetition coding (RC), spatial multiplexing (SMP), and spatial modulation (SM) [8]. These techniques differ in their strengths and

applications. Due to its diversity gains, RC is highly robust against varying transmitter-receiver alignments, making it effective in challenging environments. However, since RC does not provide spatial multiplexing gains, achieving high spectral efficiency with this method requires large signal constellations. In contrast, SMP can achieve higher data rates by leveraging multiplexing gains, but it relies on low channel correlation to realize these benefits. SM, on the other hand, combines MIMO and digital modulation techniques, offering better robustness to high channel correlation compared to SMP, while also enabling greater spectral efficiency than RC. In practical communication systems, the choice of a MIMO scheme depends on various factors, including system requirements, channel conditions, and performance goals [9,10]. Each MIMO scheme has its distinct advantages and trade-offs, making them suitable for different scenarios. SMP is optimal for environments with low channel correlation where high data rates are needed, while SM and RC excel in scenarios requiring robustness or greater spectral efficiency. A flexible approach, such as switching between different MIMO schemes, is crucial for optimizing performance under varying conditions. As such, MIMO recognition is an essential first step to enable adaptive switching between techniques, ensuring that the strengths of each MIMO scheme can be fully utilized in different environments.

MIMO fingerprints represent the intrinsic characteristics of the transmission method, primarily influenced by the number of channels and their correlations. These fingerprints are inherently challenging to replicate, and by extracting these features, we can accurately identify targets. This capability is crucial for applications such as MIMO detection and MIMO demodulation [11]. Recent advancements in artificial intelligence and machine learning, especially deep learning, have provided strong theoretical foundations for MIMO fingerprint recognition. However, most supervised learning approaches for MIMO fingerprint recognition are based on the closed-world assumption, where it is presumed that all emitter classes in the test data are already included in the training set. This assumption becomes problematic in dynamic and open environments. To address this, an open-set MIMO recognition method is proposed in this study, enabling effective MIMO recognition across the entire receiving

¹School of Microelectronics and Communication Engineering, Chongging University, Chongging 400044, China

²Department of Electrical and Computer Engineering, National University of Singapore, 117576, Singapore

³Department of Engineering, University of Cambridge, 9 JJ Thomson Avenue, Cambridge CB3 0FA, UK

⁴c.chen@cqu.edu.cn

⁵zhihong.zeng@cqu.edu.cn

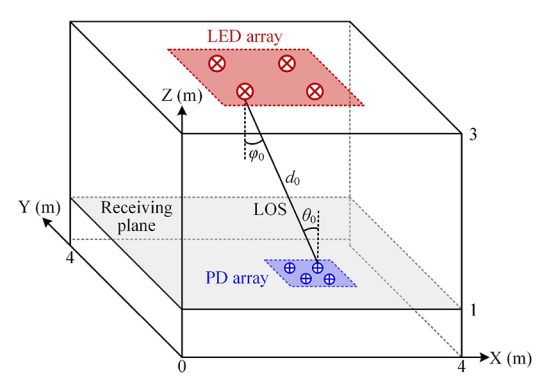


Fig. 1. Geometric setup of a general MIMO-OWC system.

plane by training with only a few fixed positions. This approach allows for fast and efficient MIMO recognition in practical OWC scenarios where data from the whole receiving plane is either unavailable or difficult to collect.

Siamese neural network (SNN) is particularly well-suited for this task due to its ability to learn and capture similarities and dissimilarities within input data [12]. This feature is beneficial for classifying MIMO fingerprints at different locations. Although the SNN has been applied to open-set recognition problems in communication, their application in OWC has not yet been explored. In this Letter, we propose an open-set MIMO recognition approach for OWC using the SNN. By sampling from a few location points on the receiving plane, MIMO schemes adopted can be well predicted for the entire receiving plane. Simulations are performed to evaluate and compare the performance of different deep learning classifiers such as the SNN and convolutional neural network (CNN) with traditional classifiers including random forest (RF), decision tree (DT), and support vector machine (SVM).

Figure 1 illustrates the geometric setup of a general MIMO-OWC system within a typical indoor environment, where a LED array with N_t LEDs is mounted in the ceiling and a photodetector (PD) array with N_r PDs is located at the receiving plane. Considering that various MIMO transmission schemes such as RC, SMP, and SM might have very distinctive performance at different positions over the receiving plane, it is efficient to apply adaptive MIMO transmission for a given receiving position so as to achieve the optimal transmission performance by selecting the most suitable MIMO transmission scheme [13]. The schematic diagram of the adaptive MIMO-OWC system with intelligent open-set MIMO recognition is depicted in Fig. 2, where insets (a), (b), and (c) show the 4×4 MIMO-OWC transmitter using RC, SMP, and SM, respectively. Letting x denote the transmitted signal vector after adaptive MIMO mapping at the transmitter side, the received signal vector at the receiver side can be expressed by the following:

$$y = Hx + n, (1)$$

where **H** is the $N_r \times N_t$ MIMO channel matrix and **n** is the additive noise vector.

In a typical indoor environment, assuming each LED follows a Lambertian radiation pattern. There are two main link models, i.e., line-of-sight (LOS) link and non-line-of-sight (NLOS) link. In this Letter, we only consider the LOS link as it occupies more than 95% of the total received power. Moreover, the PD is assumed to point vertically upward. Therefore, the channel gain

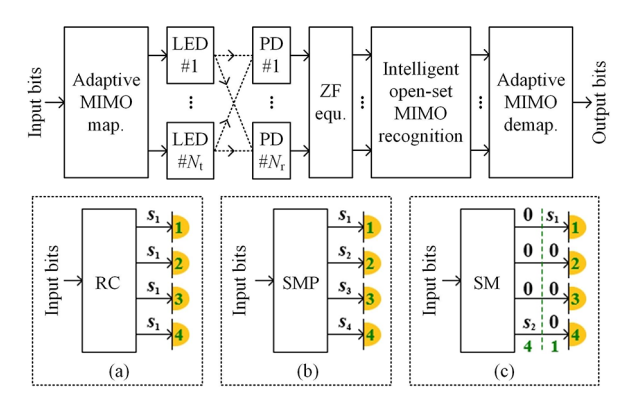


Fig. 2. Schematic diagram of the adaptive MIMO-OWC system with intelligent open-set MIMO recognition. Insets: 4×4 MIMO-OWC transmitter using (a) RC, (b) SMP, and (c) SM.

between the *r*-th PD and the *t*-th LED with $r = 1, 2, ..., N_r$ and $t = 1, 2, ..., N_t$ can be calculated by the following:

$$h_{rt} = \frac{(m+1)\rho A}{2\pi d_{rt}^2} \cos^m(\varphi_{rt}) T_s(\theta_{rt}) \theta_{rt}) \cos(\theta_{rt}), \qquad (2)$$

where $m = -\ln 2/\ln(\cos(\Psi))$ is the Lambertian emission order and Ψ is the semi-angle at half power of LED; ρ and A are the responsivity and the active area of PD, respectively; d_n is the distance between the r-th PD and the t-th LED; φ_n is the emission angle; θ_n is the incident angle; and $T_s(\theta_n)$ and $g(\theta_n)$ are the gains of optical filter and lens, respectively. Moreover, the additive noise can be modeled as a real-valued zero-mean additive white Gaussian noise with power $P_n = N_0 B$, where N_0 is the noise power spectral density (PSD) and B is the signal bandwidth. At the receiver side, zero-forcing (ZF)-based MIMO de-multiplexing is generally adopted to obtain the estimate of the transmitted signal vector \mathbf{x} , which is given by the following:

$$\hat{\mathbf{x}} = \mathbf{H}^{\dagger} \mathbf{y} = \mathbf{x} + \mathbf{H}^{\dagger} \mathbf{n}, \tag{3}$$

where $\mathbf{H}^{\dagger} = (\mathbf{H}^*\mathbf{H})^{-1}\mathbf{H}^*$ is the pseudo inverse of \mathbf{H} . After ZF equalization, intelligent open-set MIMO is first executed to recognize the adopted MIMO scheme and then adaptive MIMO demapping is performed to obtain the output bits.

To enable adaptive switching between different MIMO schemes, accurate MIMO recognition is essential. To train a MIMO recognition model, different samples need to be collected. In real-world OWC tasks, the collection of training samples often faces limitations due to various practical factors. This makes it challenging to cover all possible classes when training a recognizer or classifier. A more realistic scenario involves open-set recognition, where the training phase has incomplete knowledge of the world, and during testing, the algorithm may encounter new, unseen classes. This requires the system not only to accurately classify known classes but also to effectively handle unknown ones. Therefore, in this study, the open-set MIMO recognition using SNN is proposed.

As a metric learning-based few-shot method, the SNN utilizes the same embedding network to extract image-level features and map the images into vectors. It then employs a learnable metric to compute the absolute difference between the two vectors, representing the similarity between the two images. During training, the SNN takes in a pair of samples instead of individual samples. Each sample pair is assigned a label 1 if the images belong to the same class and 0 if they belong to different classes. The

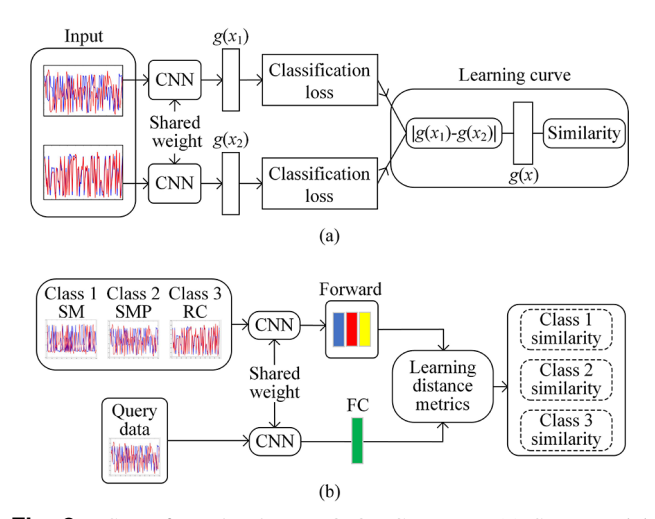


Fig. 3. SNN for a 2×2 MIMO-OWC system: (a) SNN model structure and b) SNN model structure under the episodic training strategy.

model is trained using the cross-entropy loss function. In the testing phase, sample pairs are input, and the class of a query sample is determined by identifying which reference sample has the highest similarity, thus completing the classification.

Figure 3(a) demonstrates the SNN model structure for a 2×2 MIMO-OWC system. The SNN essentially uses the same feature embedding network for a pair of inputs (x_1, x_2) . Here, x_1 and x_2 represent the received signals for N_{slot} time slots, each with a dimension of $N_{\text{PD}} \times N_{\text{slot}}$. For a 2×2 MIMO-OWC system, $N_{\text{PD}} = 2$. First, both inputs pass through the same CNN to output feature maps. After applying the flatten operation, the multi-dimensional feature maps are flattened into single vectors $[g(x_1), g(x_2)]$. A learnable metric is then used to compute the similarity between the samples. This metric involves calculating the induced distance between $g(x_1)$ and $g(x_2)$ using fully connected layers, followed by a sigmoid activation function for prediction. The formula for calculating the similarity between two inputs in a SNN is given by the following:

$$D(x_1, x_2) = \sigma\left(\sum_j \alpha_j \left| g^j(x_1) - g^j(x_2) \right| \right), \tag{4}$$

where σ represents the activation function, specifically the sigmoid activation function in this case, and α_j refers to parameters learned by the model during training, used to weigh the importance of the component distances. The last fully connected layer introduces a metric into the learned feature space from the previous layer. After passing through the activation function, it produces the similarity score for the global feature vectors of (x_1, x_2) .

Currently, most metric-based few-shot learning methods utilize an episodic training strategy to train and pre-test the model. In this study, the SNN adopts this strategy to tackle few-shot learning tasks. Figure 3(b) illustrates the model structure of the SNN under a three-way one-shot task using the episodic training strategy. In the figure, the support set consists of three classes, each containing one sample. After passing through the embedding space, the feature mappings for both the support set and query set samples are obtained. The multi-dimensional feature mappings are flattened into one-dimensional vectors via the flatten operation. Then, a learnable metric module is applied

Table 1. Parameters for the System

Parameter	Value
Room dimension	$4 \text{ m} \times 4 \text{ m} \times 3 \text{ m}$
LED positions for 2×2 MIMO	(1 m, 2 m, 3 m), (3 m, 2 m, 3 m)
LED positions for 4 × 4 MIMO	(1 m, 1 m, 3 m), (3 m, 1 m, 3 m) (1 m, 3 m, 3 m), (3 m, 3 m, 3 m)
Height of receiving plane	1 m
Semi-angle at half power of LED	65°
Gain of optical filter	0.9
Refractive index of optical lens	1.5
FOV of optical lens	70°
Responsivity of PD	0.53 A/W
Active area of PD	$1 \mathrm{cm}^2$
Modulation bandwidth	20 MHz
Noise power spectral density	$10^{-22} A^2 / Hz$

to calculate the similarity between the query sample and each class in the support set. A non-parametric nearest neighbor classifier is used to complete the classification. The model is trained end-to-end using the cross-entropy loss function. Throughout the entire training and prediction process, the SNN aims to learn a task-appropriate feature representation and perform similarity measurement in the feature space to facilitate effective classification.

In order to validate the performance of the proposed open-set MIMO recognition method with SNN, simulations are carried out by considering MIMO-OWC systems in practical indoor environments. In our simulations, MATLAB is used as the simulator, and we consider an indoor environment with a dimension of $4 \text{ m} \times 4 \text{ m} \times 3 \text{ m}$. The geometric setup of the MIMO-OWC system is depicted in Fig. 1. The LEDs are mounted on the ceiling, and the user is situated on the receiving plane. The LEDs are oriented vertically downward, while the PDs are oriented directly upward toward the ceiling. Moreover, we consider four numbers of training positions, i.e., 4, 9, 16, and 25, to evaluate the performance of the SNN-based intelligent open-set MIMO recognition method across the overall receiving plane in the indoor MIMO-OWC system, where these training positions are assumed to have a square layout, which are uniformly distributed over the receiving plane. For example, with four sampling points, we generate 2000 received signal matrices for each point, each having dimensions of $N_{PD} \times N_{slot}$, to train the SNN model. For the remaining 1600 testing points on the receiving plane, the corresponding received signal matrices are used to evaluate the accuracy. The key simulation parameters are provided in Table 1.

Figure 4 evaluates the MIMO recognition accuracy versus the transmitted signal-to-noise ratio (SNR) using various recognition methods for different numbers of training positions and MIMO setups. Specifically, Figs. 4(a)–4(d) demonstrate the recognition accuracy for a 2×2 MIMO system using 4, 9, 16, and 25 training positions, respectively, while Figs. 4(e)-4(h) illustrate the recognition accuracy for a 4 × 4 MIMO system using 4, 9, 16, and 25 training positions, respectively. The overall trend across the eight cases demonstrates that the SNN consistently outperforms the CNN and traditional machine learning techniques. In general, the SNN provides the best recognition performance, followed by the CNN, while traditional machine learning lags behind. Additionally, the recognition performance of the 2×2 MIMO system is better than that of the 4×4 MIMO system at lower SNR levels. Deep learning models, such as the SNN and CNN, achieve a 100% recognition accuracy in all

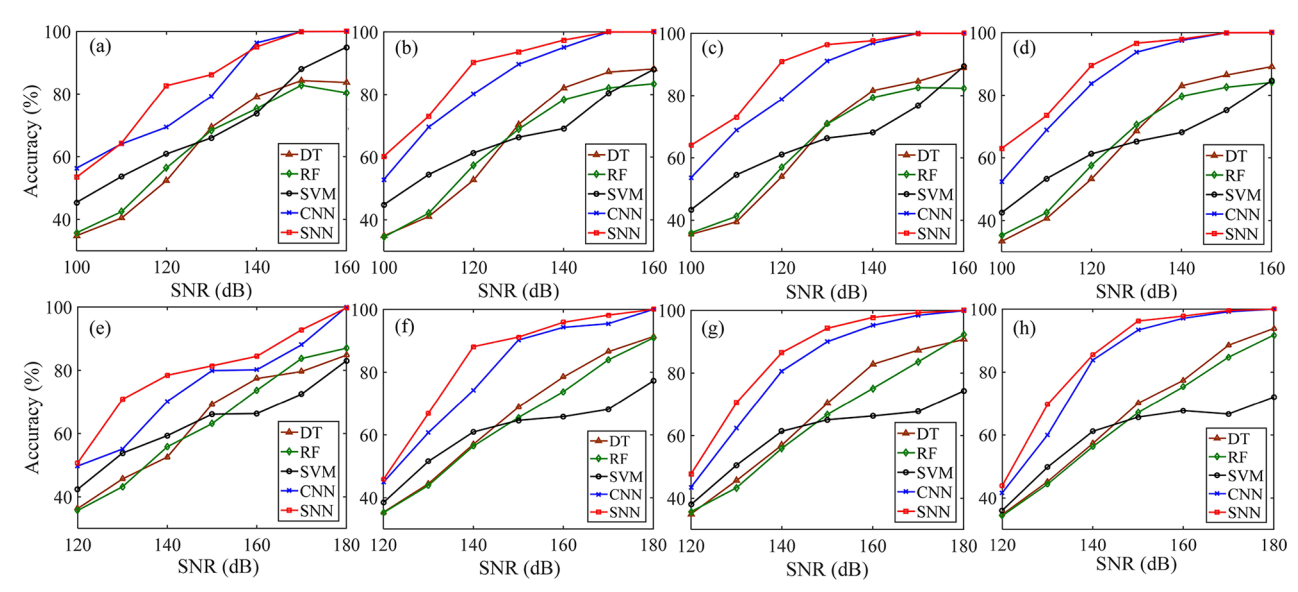


Fig. 4. Recognition accuracy versus transmitted SNR using various recognition methods for different numbers of training positions and MIMO setups: (a) 2×2 MIMO, 4 positions; (b) 2×2 MIMO, 9 positions; (c) 2×2 MIMO, 16 positions; (d) 2×2 MIMO, 25 positions; (e) 4×4 MIMO, 4 positions; (f) 4×4 MIMO, 9 positions; (g) 4×4 MIMO, 16 positions; and (h) 4×4 MIMO, 25 positions.

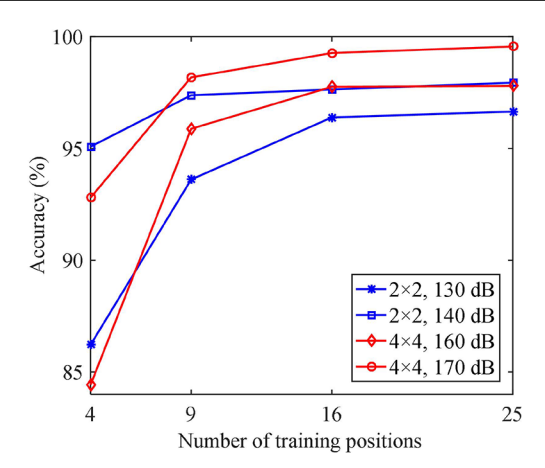


Fig. 5. Recognition accuracy versus number of training positions for various SNR values and MIMO setups when the SNN is adopted.

scenarios when the transmitted SNR reaches 160 dB and 180 dB for 2×2 and 4×4 MIMO setups, respectively.

Figure 5 illustrates the MIMO recognition accuracy versus the number of training positions for various SNR values and MIMO setups when the SNN is adopted. This comparison highlights how varying the number of training positions impacts the recognition accuracy. As observed, the accuracy improves with an increasing number of training positions, though the rate of improvement gradually slows. Notably, once the number of training positions reaches 9, the recognition accuracy exceeds 90% across all scenarios, and the recognition accuracy remains stable when more than 16 training positions are selected. It demonstrates that a relatively small number of training positions is sufficient for accurately recognizing various MIMO schemes at the receiver side, thus enabling open-set MIMO recognition across the overall receiving plane in the indoor MIMO-OWC system.

In this Letter, we have proposed and investigated an intelligent open-set MIMO recognition method for MIMO-OWC systems. Specifically, the SNN is utilized to successfully realize MIMO recognition across the overall receiving plane by selecting only a few fixed positions for training. Simulation results demonstrate that the SNN provides the best recognition performance among various recognition methods such as the DT, RF, SVM, and CNN. It is shown that the recognition accuracy improves as the number of training positions increases for both 2×2 and 4×4 MIMO-OWC systems using the SNN for MIMO recognition, and a total of 16 training positions can result in satisfactory recognition performance across the overall receiving plane. Therefore, the proposed SNN-based intelligent open-set MIMO recognition method can be promising for enabling intelligent MIMO-OWC systems in practical indoor applications.

Funding. National Natural Science Foundation of China (62271091, 61901065); Natural Science Foundation of Chongqing Municipality (cstc2021jcyj-msxmX0480).

Disclosures. The authors declare no conflicts of interest.

Data availability. Data underlying the results presented in this Letter are not publicly available at this time but may be obtained from the authors upon reasonable request.

REFERENCES

- 1. X. You, C.-X. Wang, J. Huang, et al., Sci. China Inf. Sci. 64, 1 (2021).
- 2. C.-H. Yeh, L.-Y. Wei, and C.-W. Chow, Sci. Rep. 7, 15846 (2017).
- S. Rajagopal, R. D. Roberts, and S.-K. Lim, IEEE Commun. Mag. 50, 72 (2012).
- 4. A. Ren, H. Wang, W. Zhang, et al., Nat. Electron. 4, 559 (2021).
- 5. A. Ahmad, D.-y. Choi, and S. Ullah, Sci. Rep. 12, 3608 (2022).
- 6. W. Niu, Z. Xu, W. Xiao, et al., J. Lightwave Technol. 40, 5031 (2022).
- P. F. Mmbaga, J. Thompson, and H. Haas, J. Lightwave Technol. 34, 1254 (2015).
- 8. T. Fath and H. Haas, IEEE Trans. Commun. 61, 733 (2012).
- 9. C. Chen, H. Yang, P. Du, et al., IEEE Syst. J. 14, 3202 (2020).
- 10. X. Guo, X. Li, and R. Huang, Chin. Opt. Lett. 15, 110604 (2017).
- C. Chen, L. Zeng, X. Zhong, et al., IEEE Photonics J. 14, 7302306 (2022).
- 12. D. Chicco, Artif. Neural Netw. 2190, 73 (2021).
- C. Chen, X. Zhong, S. Fu, et al., J. Lightwave Technol. 39, 6063 (2021).